Dielectric and EPR Measurements of a Main-Chain Liquid Crystalline Polyazine. Advanced Tools To Study Thermal Behavior

José Antonio Puértolas

Dpto. Ciencia de Materiales, Instituto de Ciencia de Materiales de Aragón, Centro Politécnico Superior, Universidad de Zaragoza-C.S.I.C., 50015-Zaragoza, Spain

Pablo J. Alonso

Dpto. Física de la Materia Condensada, Instituto de Ciencia de Materiales de Aragón, Facultad de Ciencias, Universidad de Zaragoza-C.S.I.C., 50009-Zaragoza, Spain

Luis Oriol and Jose Luis Serrano*

Dpto. Química Orgánica, Instituto de Ciencia de Materiales de Aragón, Facultad de Ciencias, Universidad de Zaragoza-C.S.I.C., 50009-Zaragoza, Spain

Received November 28, 1991; Revised Manuscript Received June 15, 1992

ABSTRACT: Studies of a nematic main-chain polyazine by means of differential scanning calorimetry (DSC), dielectric relaxation spectroscopy, electron paramagnetic resonance (EPR), and viscosimetry are reported in order to characterize its thermal behavior. The conductivity contribution to dielectric measurements and the temperature-induced variation of paramagnetic units seen by EPR spectroscopy suggest the thermal generation of active intermediates. Changes in polymer inherent viscosity on heating show an increase in the degree of polymerization in the solid state.

Introduction

There is at present considerable interest in the study of the motions of the dipolar grouping of liquid crystal (LC) polymers over wide ranges of frequency and temperature by means of dielectric relaxation spectroscopy. Most dielectric studies have concentrated on side-chain[1,2] and combined side groups main-chain LC polymers.[3,4] However, there are few studies of the relaxation processes in mesophases of LC main-chain polymers.[5-7] In these polymers, optical microscopy (OM) and differential scanning calorimetry (DSC) are the most usual characterization techniques.[8] Generally the thermal behavior of main-chain liquid crystalline polymers is complicated and DSC curves are difficult to explain. In some cases, dielectric measurements can give additional information about the phase transitions of these materials.

Moreover, if the phase transition temperatures are high enough, new effects appear as a consequence of the thermal cleavage of the weakest bonds. This thermal cleavage involves the formation of two fragments. The fragments could be free charges (heterolytic cleavage) or free radicals (homolytic cleavage). These active intermediates could react to increase the molecular weight of the polymer. In order to study these processes electron paramagnetic resonance (EPR) and viscosimetry measurements can be carried out. The EPR technique is specially sensitive and permits the detection of free radicals generated in homolytic cleavages, while viscosimetry studies provide confirmation of the increase in the degree of polymerization.

Recently we have synthesized in our laboratories a new family of main-chain LC polyazines.[9,10] This paper deals with a member of this new series of polymers:

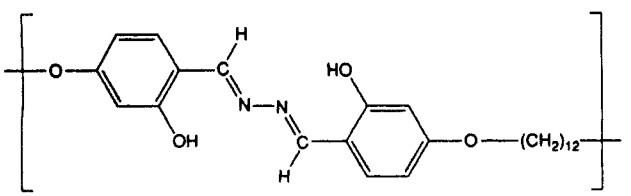

This LC polymer has a wide variety of phase transitions and is a good example for the study of the previously-mentioned problems. So we have carried out a wide study of the polymer by OM, DSC, dielectric measurements, EPR spectroscopy, and viscosimetry. Samples with different, but controlled, thermal histories have been used in order to compare the results obtained by the different techniques.

A detailed report of the results is presented in this paper. The modifications of different physical properties (dielectric constant and EPR spectra) at the temperatures T_g and T_m are given special attention.

Experimental Section

The synthesis of the polyazine was carried out by using a previously described method.[9] Intrinsic viscosity $[\eta] = 0.59$ dL/g was determined at 40 °C by using freshly prepared solutions in methanosulfonic acid as a solvent in a Cannon-Fenske viscosimeter.

Two samples with different thermal histories were prepared in order to carry out the DSC, EPR, and dielectric studies. Sample 1A was used as prepared and sample 1B was annealed at 180 °C for 1 h.

Optical microscopy (OM) was carried out by using a polarizing microscope NIKON fitted with a Mettler FP82 heating stage, a FP80 control unit, and a REICHERT-THERMOVAR, which allowed mechanical stress of the sample.

DSC measurements were performed in a Perkin-Elmer DSC-7 at a scanning rate of 5 °C/min. DSC transition temperatures were read at the maximum of the peaks.

Dielectric measurements were carried out by using a two-terminal dielectric cell, described elsewhere, and a computer-controlled General Radio 1689 Digital bridge for measuring the electric impedance of the capacitor. The sample was held between the condenser plates (golden brass circular electrodes, diameter 12 mm) with the aid of a PTFE annular ring spacer (500-μm thickness). The frequency range was 100–10^5 Hz. The heating rate was about 5 °C/min.

EPR spectra were measured with a Varian E-122 spectrometer working in X-band. For measurements above room temperature (RT) the variable-temperature accessory (E-265) from Varian was used. The powdered samples were placed inside a quartz tube and the temperature was monitored by a copper–constantan

0024-9297/92/2225-6018$03.00/0

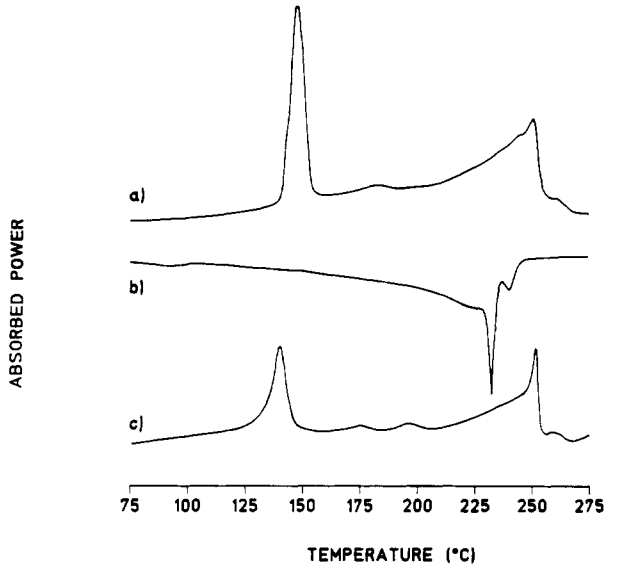

Figure 1. DSC traces of samples with different thermal treatment: (a) first heating run of sample 1A; (b) first cooling run of sample 1A; (c) first heating run of sample 1B. Scanning rate = 5 °C/min.

thermocouple attached to the tube. The error in temperature was estimated to be about 0.5 °C and its stability was better than 0.2 °C.

Results and Discussion

OM and DSC Measurements. Optical microscopy showed a biphase mesophase–isotropic liquid between 252 and 260 °C at the heating run. On cooling the isotropic melt, a grainy texture began to appear at 252 °C. As described elsewhere[9] the mesophase was identified as nematic by means of miscibility studies with a nematogenic compound. Below 230 °C the sample did not flow and remained unchangeable up to room temperature.

As can be seen in Figure 1a, sample 1A showed a sharp first-order transition at 150 °C, which could be due to a C–C′ transition. The melting and isotropization processes appear as a broad complex region between 195 and 270 °C. The broadness of this region is attributed to the polydispersity of the unfractionated polymer. The maximum of the peak, 251 °C, can be assigned to T_m and T_i appears as a shoulder at 262 °C. On cooling (Figure 1b) it is worth noting that a supercooling occurs for the isotropic liquid–mesophase and mesophase–crystal transitions. The former appears as a peak at 241 °C and the latter as a sharp peak at 233 °C. No first-order transitions were observed below 233 °C. The C–C′ transition disappeared during the second heating.

The DSC curves of the annealed sample 1B are very similar to the curves of sample 1A (polymer as prepared) but some differences can be observed in the first heating run (figure 1c): a smaller C–C′ transition at a lower temperature and a narrowing of the melting and isotropization region. This narrowing can be attributed to a smaller polydispersity of both chain length and crystal size in the annealed sample. However, the maximum of the peak corresponding to T_m and the isotropization shoulder appear at the same temperatures. The cooling scan and successive heating scans were identical with those of sample 1B.

Besides, some decomposition was observed in the isotropic state.

In order to study the glass transition that characterizes the amorphous region of this semicrystalline polyazine, a sample was quenched from the isotropic melt to liquid nitrogen and annealed at 60 °C overnight. Figure 2 shows the T_g region as observed on heating (heating rate = 40 °C/min). The glass transition temperature, T_g = 89 °C, corresponds to the half-devitrification point. The shape of the glass transition indicates a pre-glass transition or even two separate glass transitions, as have been described previously by Cheng et al.[11-14]. Furthermore, an enthalpy relaxation endotherm appears because of annealing close to T_g.[15] The glass transition was not observed in the heating run of the samples as polymerized (sample 1A) but on cooling a shift of the baseline at 97 °C (Figure 1b) can be observed. The difference between the two measured T_gs could be due to their different thermal histories.

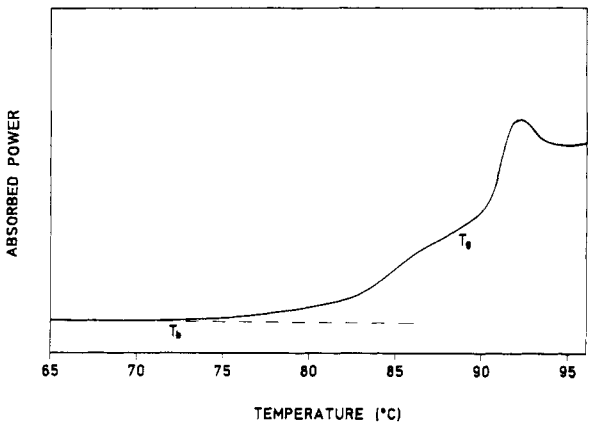

Figure 2. DSC trace in the glass transition region. For analysis see text.

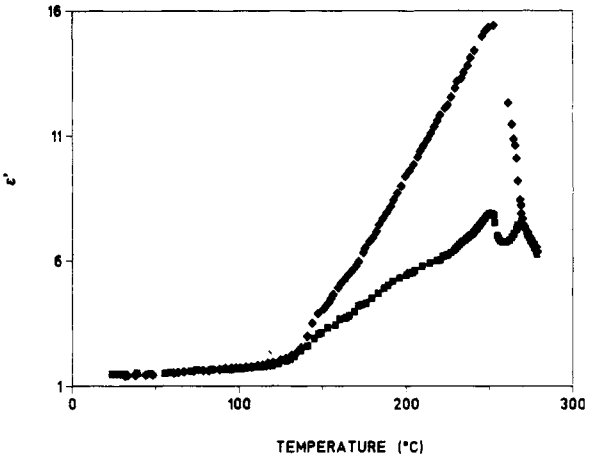

Figure 3. Temperature dependence of real part, ϵ', of the complex dielectric function at 1 kHz: (♦) sample 1A; (■) sample 1B.

Dielectric Measurements. Dielectric measurements of the complex permittivity $\epsilon^*(T) = \epsilon'(T) - i\epsilon''(T)$ were carried out from room temperature (RT) to 280 °C, at a frequency of 1 kHz and a voltage of 1 V rms, on 1A and 1B samples. The results obtained allow an improved definition of the polymer transition temperatures. Figures 3 and 4 show the real part of the permittivity and dielectric loss dependence on temperature for the two samples, respectively.

In both samples the measurements exhibit, at room temperature, low values of the real part of the permittivity, ϵ', according to the dipolar structure of the polymer. In any case, we want to point out that we intend to focus our attention on the evolution of the permittivity with temperature as well as with frequency, bearing in mind that the absolute values can be affected by errors associated with this type of technique. The dielectric loss factor, ϵ'', at this temperature is negligible. When the samples are heated, the complex permittivity remains constant up to

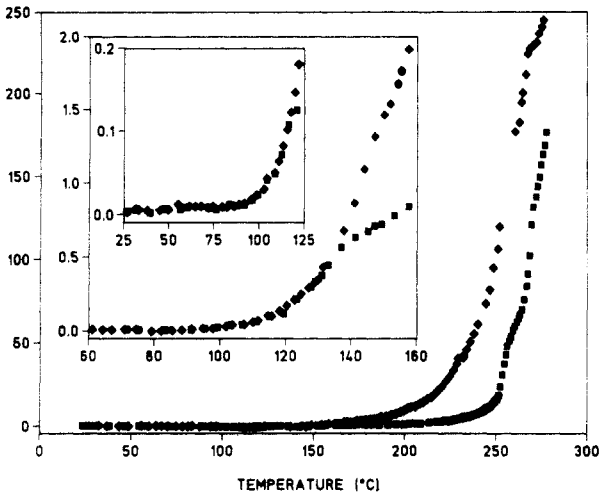

Figure 4. Temperature dependence of dielectric loss factor, ϵ'', at 1 kHz: (♦) sample 1A; (■) sample 1B. Internal frames show C–C′ and glass transition regions.

below 100 °C. Above this temperature, $\epsilon''(T)$ increases rapidly, which is more marked as the temperature increases. The beginning of this increase is associated with the glass transition, T_g, of the amorphous part of this semicrystalline polymer, since it coincides with the step observed in the DSC measurements. The dielectric techniques are more accurate, however, since there is no need to quench the sample from its isotropic phase. The free volume increase associated with T_g introduces more molecular mobility for the dipoles and ions and is reflected in the $\epsilon''(T)$ rise observed. The value of $\epsilon'(T)$ remains practically constant up to 140 °C, and then shows stepwise behavior, at this temperature, coinciding with the transition C–C′ noticed in DSC measurements.

Above 140 °C, $\epsilon'(T)$ rises sharply, reaching a maximum at 250 °C. This peak, T_m, is preceded by a wide shoulder, in the same region where DSC shows complex behavior. It is associated with molecular weight distribution of unfractionated samples which is also reflected in the lower values of ϵ' and ϵ'' in sample 1B. In this sample the nematic phase appears in $\epsilon'(T)$, associated with a plateau between two maxima, 250 and 270 °C. The second maximum coincides with the nematic–isotropic transition, detected by a small peak, at approximately 270 °C, in DSC measurements. Sample 1A presents, however, a strong decrease in $\epsilon'(T)$ from the maximum until the value observed for sample 1B in the isotropic phase is reached.

Both, T_m and T_{NI} are seen in $\epsilon''(T)$, by means of slope changes in the monotone rise, above 200 °C.

A final analysis of the thermal evolution of $\epsilon^*(T)$, in particular $\epsilon''(T)$, indicates the absence of a Debye relaxation process in the overall range of temperature. This behavior leads us to consider the presence of a thermally activated ac conductive phenomenon. In order to analyze this behavior in detail, dielectric measurements as a function of frequency, $\epsilon^*(\omega) = \epsilon'(\omega) - i\epsilon''(\omega)$, were carried out in the range 100 Hz–100 KHz, at constant temperature, in the different phases observed in the polyazine.

The results show that $\epsilon''(\omega)$ has three different behaviors depending on temperature. Below about 110 °C ϵ'' is negligeable and frequency independent. Above this temperature the curve log ϵ'' versus log ω (Figure 5) is characterized by the superposition of two process: a conductivity contribution and a wide and weak relaxation process. Because of the temperature range in which it appears, it could be associated with α processes in a semicrystalline polymer. However, there are not enough data to study it separately. At a high enough temperature

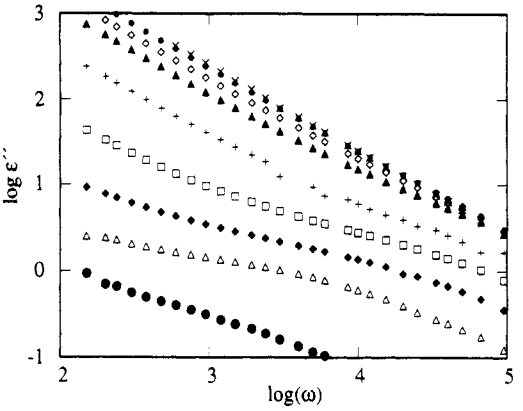

Figure 5. Dependence of ϵ'' as a function of the frequency ω for sample 1A measured at different temperatures: 127.7 °C (●), 150.0 °C (△), 174.9 °C (♦), 199.6 °C (□), 230.4 °C (+), 252.8 °C (▲), 261.4 °C (◇), 269.2 °C (●), and 279.4 °C (x).

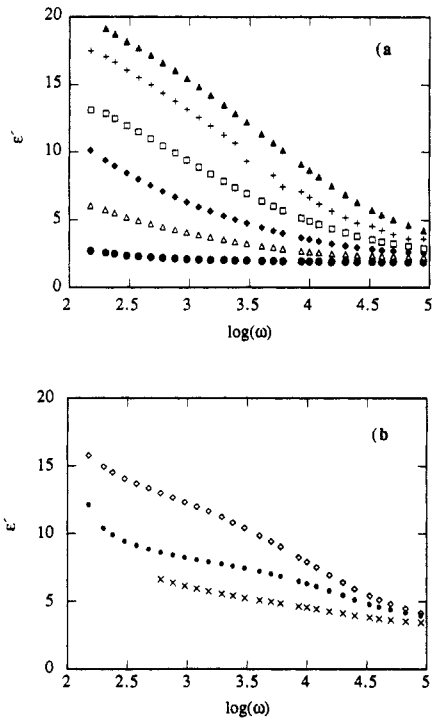

Figure 6. Evolution of the real part of the dielectric constant ϵ' as a function of the frequency at different temperatures: (a) 127.7 °C (●), 150.0 °C (△), 174.9 °C (♦), 199.6 °C (□), 230.4 °C (+), and 252.8 °C (▲); and (b) 261.4 °C (◇), 269.2 °C (●), and 279.4 °C (x).

the relaxation contribution shifts at frequencies above 100 KHz, showing mainly the conductive process, which is practically independent of the temperature above the nematic–isotropic transition.

The analysis of $\epsilon'(\omega)$ indicates that is displays similar behavior to $\epsilon''(\omega)$. So, below 100 °C, the permittivity ϵ' is practically frequency independent. The two formerly described processes in ϵ'' also produce a considerable increase in ϵ' as frequency decreases (Figure 6). However, while ϵ'' goes on slowly increasing at temperatures above the melting temperature the permittivity ϵ' tends to decrease. Since in this temperature range the relaxation process shows a shift toward frequencies higher than 100 KHz, ϵ' might be sensitive to this evolution. In any case, at present we are unable to account for such behavior.

Figure 7 shows the real part of the complex conductivity $\sigma^* = i\omega\epsilon^* = \sigma_1 + i\sigma_2$ versus the reciprocal temperature (1000/T). In this plot the last three regions are more clearly represented. At low temperatures the thermal activation

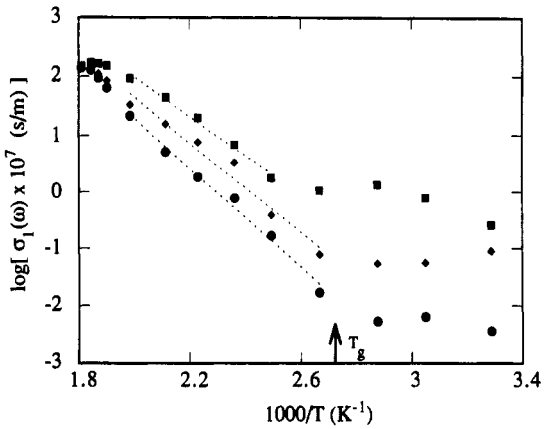

Figure 7. Plot of the log of the real part of the conductivity σ_1 as a function of the reciprocal absolute temperature ($1000/T$) (K^{-1}) at different frequencies: 1 kHz (●), 10 kHz (♦), and 100 kHz (■).

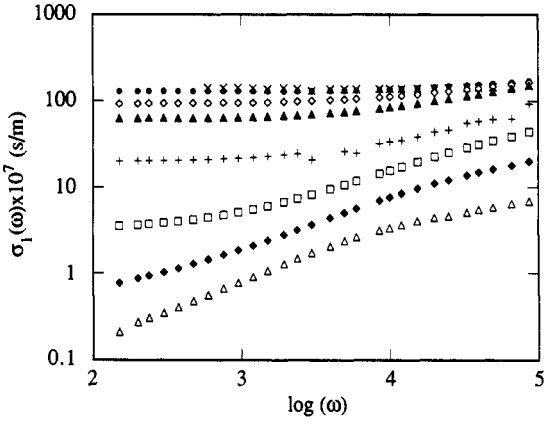

Figure 8. Frequency dependence of σ_1, measured at different temperatures: 150.0 °C (△), 174.9 °C (♦), 199.6 °C (□), 230.4 °C (+), 252.8 °C (▲), 261.4 °C (◊), 269.2 °C (●), and 279.4 °C (x).

of the conductivity is almost negligible. However, above a critical temperature an Arrhenius-type process is activated, increasing considerably the conductivity. The extrapolation of this critical temperature at low frequencies coincides with the glass transition obtained from the DSC measurements (marked by an arrow in Figure 7), which permits us to correlate this thermal activated process with the increase in the mobility of carriers in the polymer.

Figure 8 represents log σ_1 versus log ω at different temperatures. An analysis of the data indicates that $\sigma_1(\omega)$ can be expressed by means of the relation $\sigma_1(\omega) = \sigma_1(0) + A\omega^s$, with $\sigma_1(0)$, A, and s depending on the temperature. The former term is frequency-independent and it is identified with the dc conductivity. The latter is purely dispersive and corresponds to a hopping conductivity of the charge carrier[16] in a similar way to amorphous or disordered conductors.[17,18]

Fitting our data to the last equation, we obtain values of s between 0.2 and 0.5, with a negative temperature dependence. The dc conductivity presents a temperature dependence in accordance with an Arrhenius law $\sigma_1(0) = B\exp(-Q/RT)$ (Figure 9), with an activation molar energy Q = 11.5 kcal/mol, in the range 150–270 °C. Below these temperatures, the results do not allow extrapolation of the ac conductivity at low frequency to obtain $\sigma_1(0)$.

This conductivity could be due to extrinsic ionic impurities, although the polymerization method did not lead us to consider this possibility. Moreover, in this case the thermal behavior described seems to point to the presence of the thermally-activated ionic dissociation process. From the activation molar energy, Q, it is rather

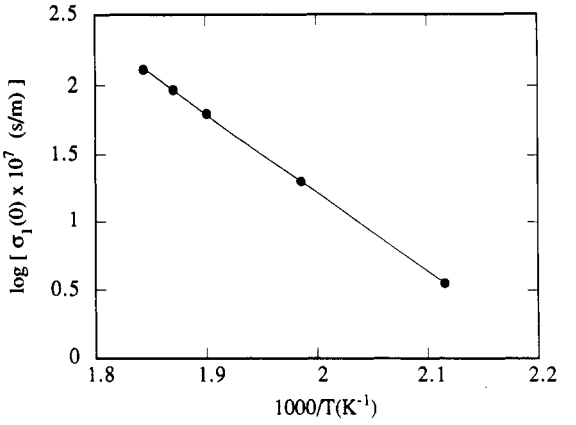

Figure 9. Extrapolated dc conductivity, $\sigma_1(0)$, for sample 1A versus inverse temperature ($1000/T$) (K^{-1}).

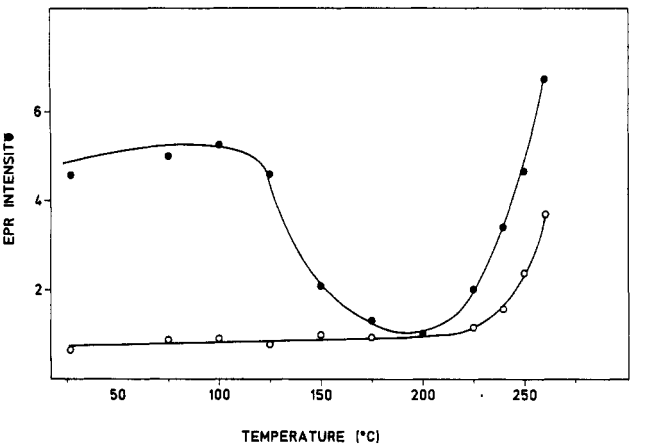

Figure 10. Intensity of the $g \approx 2$ EPR signal as a function of the temperature: (●) sample 1A; (○) sample 1B.

difficult to evaluate the dissociation energy, E. Both energies, Q and E, are related by a factor 2 due to the application of the mass action law to the dissociation process and also to the correction due to the reduction of Coulombic forces between ions in a dielectric medium. The estimation of this energy, from data, provides a lower level of approximately 70–80 kcal/mol, according to the energy related to the dissociation process expected in the end groups. In order to ascertain whether this thermally-activated process is accompanied by the generation of free radicals, EPR measurements were carried out. So we measured the EPR spectra of samples 1A and 1B at different temperatures between room temperature (RT) and 260 °C.

EPR Measurements. Before any treatment (sample 1A) a signal at $g \approx 2$ with a peak to peak width (ΔB_{pp}) of about 0.9 mT is observed when measured at RT. The observation of the same trace regardless of polymerization conditions shows that the EPR signal is inherent to the polymer and is not due to an unwanted impurity. It is associated with free radicals. Moreover, in the case of a cured sample (1B) a narrower (ΔB_{pp} = 0.7 mT) signal at the same field is also found but its intensity is about five times lower.

When the samples are heated up, modifications in their EPR signal are observed. Changes in intensity as well as in width are detected. Figure 10 represents for both samples 1A and 1B the intensity of the signal (estimated by the product of its height by the square of ΔB_{pp} and normalized to the sample weight) as a function of temperature. In the case of a treated sample the intensity of the EPR signal remains constant up to 200 °C and at higher temperatures a considerable increase is observed.

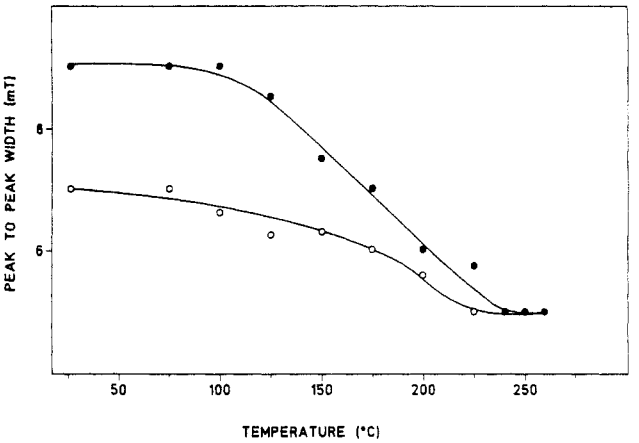

Figure 11. Peak-to-peak width of the $g \approx 2$ EPR signal as a function of the temperature: (●) sample 1A; (○) sample 1B.

In the case of untreated samples (1A) the thermal evolution of the intensity of the EPR signal is more complex. It remains practically unchanged up to 100 °C and then strongly decreases, reaching its minimum value at about 200 °C with an intensity similar to that of a cured sample. At higher temperatures the intensity of the EPR signal also increases.

As far as peak width is concerned, it can be seen (Figure 11) that in both types of samples it monotonically decreases as the temperature increases, reaching the same value (ΔB_{pp} = 0.47 mT) at temperatures above 240 °C. It is noteworthy that this width remains unchanged during a cooling process down to RT.

In order to explain this behavior, two different and competitive processes have to be considered: the increase in the degree of polymerization when thermally treated and the thermal generation of radicals at temperatures above 200 °C.

Probably, during the drying (at 80 °C for 24 h) of the polymers, some free radicals are thermally generated, mainly formed in the terminal groups. In the thermally treated polymers (sample 1B) the number of these terminal sites is lower than the untreated sample 1A due to the reaction of terminal groups to obtain a polymer with a higher degree of polymerization. This accounts for the difference in the intensity of the RT spectra of both types of sample. The decrease in the signal observed in the untreated samples between 100 and 200 °C can also be explained in the same way. The mean length of the chains increases during this thermal treatment whereas the number of terminal sites decreases. Consequently the number of free radicals also diminishes.

This process of increasing the degree of polymerization is also responsible for the irreversible narrowing of the width of the EPR signal (Figure 11). The existence of several types of terminal sites for the radicals leads to an inhomogeneous broadening of the signal. During the thermal treatment the short chains disappear and thus the distribution of sites becomes less spread out, so the EPR signal narrows.

The strong increase of radicals at temperatures higher than 200 °C is due to their formation as a consequence of a thermal process. This is related to the increase in dc conductivity $\sigma_1(0)$. This can be easily understood if, by means of thermal activation, we induce a charge separation that simultaneously gives out ions (contributing to the conductivity) and radicals (which are responsible for the EPR signal).

Viscosimetric Measurements. In order to corroborate the possibility of increasing molecular weight on heating this polyazine, a study of the polymer solution viscosity was carried out. Table I shows the effect of increasing the polymer-inherent viscosity of samples with a different thermal history: sample 1A (polymer as prepared) and samples 1B, 1C, and 1D with an isothermal heating at 180 °C for 1, 4, and 24 h, respectively. The samples treated over a long period of time showed deeper coloration and incomplete solubility in methanosulfonic acid. In the case of sample 1D only about 10% was soluble (initial concentration, 0.3 g/dL).

Table I
Changes in Polymer Solution Viscosity on Heat Treatment

sample	T, °C	time, h	η_{inh}, dL/g[a]
1A			0.62
1B	180	1	0.71
1C	180	4	0.82[b]
1D	180	24	c

[a] Concentration of 0.3 g/dL in methanosulfonic acid at 40 °C. [b] Residuum <1%. [c] Soluble fraction <10%

The inherent viscosity gain can be explained by the increase in molecular weight according to the reaction of active end groups in the solid state. Continued heating may yield an extreme degree of polymerization or cross-linking, as can be observed in sample 1D. Given the structure of the mesogenic core with two intramolecular H-bonds between hydroxylic hydrogen and the nearest nitrogen of the azine group,[19] the polymer solutions can be expected to show fluorescence.[20] In fact, the solutions of samples 1A, 1B, and 1C are fluorescent, so it can be inferred that the mesogenic units remain unchanged during the first stages of the thermal treatment. In these stages, there is an increase in the molecular weight of the linear liquid crystalline polyazine. With a stronger thermal treatment the functional groups of the mesogenic core might react to obtain a cross-linked polymer without mesogenic properties.

Conclusion

Dielectric measurements are a useful way of detecting the change that occurs at the glass transition, T_g. This transition is not easy to observe in DSC traces if the amorphous region has not been favored by thermal quenching. Above T_g, two processes are involved. The relaxation processes disappears at the melting transition, while the conductivity contribution goes on increasing. At high frequencies, this process displays a dispersive behavior similar to a hopping conductivity. The dc conductivity follows an Arrhenius law with values of activation molar energy related to a thermally-activated ionic dissociation process.

In the same way EPR measurements provide information about some processes that occur on the molecular level during the transitions. The decrease in the number of free radicals at temperatures between T_g and T_m points to combination reactions of these active intermediates, which may increase chain length. This interpretation is corroborated by viscosimetry measurements. The considerable increase in the free radical concentration above T_m correlated with the above-mentioned increase in dc conductivity suggests a thermal instability of the polymer, giving out free radicals and ions as a consequence of a thermal cleavage of some bonds.

Finally we would like to point out that both EPR and dielectric spectroscopies are quite sensitive and useful complements to the DSC technique, providing relevant

information about the thermal behavior of the studied polyazine.

Acknowledgment. This work has been partially supported by the CICYT (Spain) under the projects MAT90-0748 and MAT 89-0531-C02-02. The financial support from the Ministerio de Educacion y Ciencia (Spain) for a grant to L. Oriol is greatly appreciated.

References and Notes

(1) Haws, C. M.; Clark, M. G.; Attard, G. S. In *Side Chain Liquid Crystal Polymers*; McArdle, C. B., Ed.; Blackie: London, 1989; p 196.
(2) Vallerien, S. U.; Kremer, F.; Boeffel, C. *Liq. Cryst.* **1989**, *4*, 79.
(3) Vallerien, S. U.; Zentel, R.; Kremer, F.; Kapitza, H.; Fischer, E. W. *Makromol. Chem., Rapid Commun.* **1989**, *10*, 333.
(4) Endres, B. W.; Ebert, M.; Wendorff, J. H. *Liq. Cryst.* **1990**, *7*, 217.
(5) Araki, K.; Aoshima, M.; Namiki, N.; Ujiie, S.; Koide, N.; Iimura, K.; Imamura, Y.; Williams, G. *Makromol. Chem., Rapid Commun.* **1989**, *10*, 265.
(6) Kreese, H.; Rotz, U.; Lindau, J.; Kuschel, F. *Makromol. Chem.* **1989**, *190*, 2953.
(7) Vallerien, S. U.; Fremer, F.; Huser, B.; Spiess, H. W. *Colloid Polym. Sci.* **1989**, *267*, 583.
(8) Noel, C. In *Polymeric Liquid Crystals*; Blumstein, A., Ed.; Plenum Press: New York and London, 1985; p 21.
(9) Marcos, M.; Oriol, L.; Ros, B.; Serrano, J. L. *Mol. Cryst. Liq. Cryst.* **1988**, *155*, 103.
(10) Marcos, M.; Navarro, F.; Oriol, L.; Serrano, J. L. *Makromol. Chem.* **1989**, *190*, 305.
(11) Cheng, S. Z. D.; Janimak, J. J.; Sridhar, K.; Harris, F. W. *Polymer* **1988**, *30*, 494.
(12) Cheng, S. Z. D.; Cao, M. Y.; Wunderlich, B. *Macromolecules* **1986**, *19*, 1868.
(13) Cheng, S. Z. D.; Wunderlich, B. *Macromolecules* **1987**, *20*, 1630.
(14) Cheng, S. Z. D.; Wunderlich, B. *Macromolecules* **1988**, *21*, 789.
(15) Cheng, S. Z. D. *J. Appl. Polym. Sci., Appl. Polym. Symp.* **1989**, *43*, 315.
(16) *Hopping Conduction in Solids*; Bottger, H., Bryskin, U. V., Eds.; Verlag Akademie: Berlin, 1986.
(17) *Impedance Spectroscopy*; MacDonald, J. R., Ed.; John Wiley: New York, 1987.
(18) *Electronic Processes in Non-Crystalline Materials*; Mott, N. F., Davis, E. A., Eds.; Clarendon Press: Oxford, 1979.
(19) Elguero, J.; Jaime, C.; Marcos, M.; Meléndez, E.; Sánchez-Ferrando, F.; Serrano, J. L. *J. Mol. Struct.* **1987**, *150*, 1.
(20) Sandor, G. In *The Chemistry of the Carbon-Nitrogen Double Bound*; Patai, S., Ed.; Interscience Pub.: London, 1970; p 54.

Registry No. 1A (copolymer), 114411-94-8; 1A (SRU), 114426-83-4.